



## OPEN ACCESS

## EDITED BY

Yuanxing Xia,  
Hohai University, China

## REVIEWED BY

Yongli Ji,  
Nanjing Institute of Technology (NJIT), China  
Yixing Ding,  
Nanjing Tech University, China

## \*CORRESPONDENCE

Chunmei Zhang,  
✉ 29141592@qq.com

RECEIVED 02 January 2024

ACCEPTED 29 January 2024

PUBLISHED 15 February 2024

## CITATION

Zhang C, Jiang J, Cai C, Yu H, Yang D and Li Z (2024), Optimal economic dispatching strategy for power systems considering distributed controllable load clusters. *Front. Energy Res.* 12:1364395. doi: 10.3389/fenrg.2024.1364395

## COPYRIGHT

© 2024 Zhang, Jiang, Cai, Yu, Yang and Li. This is an open-access article distributed under the terms of the [Creative Commons Attribution License \(CC BY\)](#). The use, distribution or reproduction in other forums is permitted, provided the original author(s) and the copyright owner(s) are credited and that the original publication in this journal is cited, in accordance with accepted academic practice. No use, distribution or reproduction is permitted which does not comply with these terms.

# Optimal economic dispatching strategy for power systems considering distributed controllable load clusters

Chunmei Zhang<sup>1\*</sup>, Jiang Jiang<sup>2</sup>, Chunyuan Cai<sup>1</sup>, Hengyou Yu<sup>1</sup>, Duotong Yang<sup>3</sup> and Zhuohuan Li<sup>3</sup>

<sup>1</sup>Zhongshan Power Supply Company of Guangdong Power Grid Co., Ltd., Zhongshan, Guangdong, China, <sup>2</sup>Guangdong Power Grid Co., Ltd., Guangzhou, Guangdong, China, <sup>3</sup>Southern Power Grid Digital Grid Research Institute Co., Ltd., Guangzhou, Guangdong, China

The day-ahead dispatching of power system depends on the predicted renewable energy output and load power, which brings great challenges to the real-time power balance. This paper focuses on voltage sensitive loads (VSLs) that are widely distributed in space, thus exploring the real-time dispatching potential for VSLs. Firstly, based on the P-V relationship of VSLs clusters, a ZIP model is adopted to establish VSLs' power controllable model. Meanwhile, considering the potential voltage instability risk during the process of voltage regulation, a linear relationship between voltage safety margin (VSM) index and node power variation was derived. Then, a two-stage linear dispatching model for controllable VSLs clusters was established to meet the needs of online application. In detail, the first stage mainly focuses on evaluating the scheduling potential of VSLs clusters and the second stage determines the optimal real-time response strategy for VSLs clusters. Finally, the effectiveness and feasibility of the proposed method are verified through an improved IEEE-30 node system.

## KEYWORDS

voltage sensitive loads (VSLs), ZIP model, voltage safety margin, two-stage linear dispatching model, real-time power balance

## 1 Introduction

At present, the green transformation and low-carbon economic dispatching of the power system are the focus of the power industry (Wen et al., 2024). Urban power grids are accelerating the investment and construction process of renewable energy, and the proportion of renewable energy generation represented by wind and photovoltaic is gradually increasing (Herath and Venayagamoorthy, 2021). However, wind power output has significant fluctuations, uncertainties, and anti-peak characteristics, which pose great difficulties for the consumption of wind power. Under this background, exploring the dispatching potential of the load side, guiding the load side to participate in demand response (DR) through incentive measures can not only avoid large-scale economic investment by power grid companies, reduce peak shaving costs, but also provide flexible peak shaving resources to meet different time scale needs (Wang et al., 2018; Schneider et al., 2022). Users can also benefit from it, assisting in the consumption of renewable energy while reducing their own production electricity costs, achieving a win-win situation.

Compared to industrial loads, the adjustable load capacity in residential and commercial areas is smaller, and the effect of individual residential and commercial load participating in DR is not good. Most of them use load aggregators or agents as bridges, and after aggregation, they participate in power grid scheduling as a unified interest entity, represented by electric vehicles (EVs) and temperature control loads (TCLs). Currently, research on scheduling methods for this type of load is relatively mature. In order to reduce the negative impact of disorderly charging and discharging of large-scale EVs on the power grid, reference (Ren et al., 2022) designed a hierarchical scheduling framework, which achieves cluster control of EVs and TCLs through aggregators. Based on load scheduling instructions issued by the system side, point-to-point transactions are carried out; in reference (Rassaei et al., 2015), researchers analyzed the impact of users' electricity consumption behavior on the charging demand of EVs and established a bidding strategy suitable for the day-ahead electricity market. Distributed algorithms were used to solve the problem, achieving the goal of minimizing the electricity demand; in reference (Zeng et al., 2022), a multi-stage regulation model of the EVs was established. Through three-stage rolling optimization, the conservatism of the day-ahead regulation stage was reduced, and the power distribution scheme of the EVs' batteries was given to improve economic returns. In reference (Li et al., 2022), in order to reduce the adverse effects caused by the deviation between the expected and actual response rate of EVs, the acceptance of scheduling risks by load aggregators is divided into optimistic and pessimistic types. A robust optimization model is used to minimize the operating costs of aggregators. Reference (Kong et al., 2023) proposed a peak shaving potential evaluation model of virtual power plant based on price elasticity mechanism and consumer psychology, which fully considers market incentives and risk avoidance factors, accurately characterizes the user characteristics. Reference (Zhang et al., 2018) designed a real-time intelligent charging algorithm for EVs that integrates building energy management systems and charging equipment controllers for scheduling. Considering the rapid development of communication technology and the increase in the number of base station construction, in reference (Yong et al., 2021), the difficulties, prospects, and key technologies of 5G base stations participating in DR were analyzed. Through the collaborative scheduling of communication network and power grid, the idle energy storage equipment in the base stations was fully utilized, effectively reducing the operating costs of communication operators and the energy storage investment costs on the power grid side.

In addition, there is a large number of building loads widely distributed in residential and commercial areas. Guiding the load in the building to participate in DR can effectively alleviate the situation of electricity shortage and promote energy conservation. In reference (Faddel et al., 2022), researchers designed a coordinated scheduling scheme for multiple buildings and the power grid, provided a convex optimization model describing the heating, ventilation, and air conditioning systems of buildings, and used the alternating direction multiplier method to interact with the minimum amount of data that satisfies iterative convergence, avoiding potential risks of privacy leakage. Reference (Wei et al., 2021) proposes a data-driven adaptive dynamic programming method to solve the optimal control scheme for air conditioning inside buildings. A three-layer neural network is used to predict

environmental temperature, lighting conditions, and load demand. In reference (Shi et al., 2022), a complete system DR platform was developed for building load, and system deployment and bidirectional adaptation devices were designed and developed. Reference (Tang et al., 2023) comprehensively considers the DR of building load, the thermal comfort needs of users, and the thermal stability constraints of oil immersed transformers. Within the allowable maximum load rate range, distribution network optimization scheduling is carried out to maximize the potential of load side scheduling while considering the safety of the distribution network.

Overall, there are two main ways for residents/commercial areas to participate in peak shaving of the power system: 1) Adjusting their own electricity consumption behavior under the guidance of electricity prices. This participation method requires that electricity prices can accurately reflect the dynamic characteristics of renewable energy output and the supply-demand relationship between sources and loads, in order to accurately guide load side peak shaving and valley filling (Dai et al., 2022). When the electricity price is unreasonable, it may even further widen the peak-valley difference. Therefore, many scholars have conducted research on electricity price updates and peak-valley time division. For example, to improve the consumption capacity of photovoltaic power in the distribution network, reference (Wang et al., 2023) established a TOU electricity price optimization model that takes into account photovoltaic output characteristics and DR. References (Chen et al., 2023; Yu et al., 2023) guide the orderly use of electricity in the distribution network by dynamically updating the real-time node marginal electricity prices, ensuring the balance of interests among market participants. 2) Voluntarily participate in the peak-shaving auxiliary service market through rules such as contract agreements, bidding auctions, etc. For example, in reference (Wen et al., 2023), the electricity sales company adopts an insurance mechanism and signs a DR contract with the load side to transfer the risks caused by electricity fluctuations and uncertainty. In reference (Li et al., 2021), incentive contracts were signed between the power grid and movable loads, which can still provide practical and feasible optimal incentive schemes in scenarios of information asymmetry. Reference (Ge, 2022) proposed an adjustable resource auction method and designed a corresponding information communication framework for load side participation in services.

However, the day-ahead dispatching of power system depends on the predicted renewable energy output and load power. The uncertainty of renewable energy output and load power poses a huge challenge to the real-time power balance of power system. Unlike common adjustment loads such as EVs, TCLs, and building loads, there are also some loads in the distribution network that have fast response speed. The power consumption of these loads is closely related to the voltage of the connecting nodes, which is named as voltage sensitive loads (VSLs). This type of load is insensitive to electricity prices and has small capacity and poor adaptability, which has often been ignored in previous studies (Jin et al., 2018). Common VSLs include small electrical appliances, lighting, and public service loads that are necessary for many household users (Lezama et al., 2020). In addition, the power of the distribution network is often closely related to the voltage of root node and can also be seen as a typical type of VSLs. The participation of VSLs can achieve the goal of voltage reduction and energy conservation.

Currently, power companies such as Southern California Edison (Williams, 1995), Northeast Utilities (Lauria, 1987), Bonneville Power Administration (De Steese, 1987), BC Hydro (Dwyer et al., 1995), Northwest Energy Efficiency Alliance (Short and Mee, 2012), and Hydro Quebec achieve power control of VSLs by regulating node voltage, thus effectively alleviating power supply pressure and getting good economic results. For example, a detailed simulation study was given by the Department of Energy in 2010 shows a reduction in annual energy of 3.04% through VSLs participating in scheduling (Short and Mee, 2012; Diaz et al., 2013). Hence, this paper selects voltage sensitive loads (VSLs) to explore the potential for real-time scheduling. The way for VSLs participate in scheduling is simple, without the need for additional installation of control equipment and signing incentive agreements, which can be seen as a direct control strategy. By utilizing existing reactive power devices in the system, continuous voltage regulation can be achieved through AVC control framework, ultimately achieving power control of VSLs. It should be noted that node voltage is allowed to vary within a certain range (such as in China, voltage can vary within  $-10\%$ – $+7\%$ ), leaving room for the control of voltage sensitive loads and not affecting the user's experience, which is also a prerequisite for conducting real-time VSLs' scheduling (Tang et al., 2018). Unfortunately, there are still some challenges in the current implementation of VSL scheduling. Firstly, in terms of scheduling methods, the most widely used voltage regulation method is to install on load tap changer (OLTC) at the load connection point, and change the node voltage by adjusting the OLTC (Lv et al., 2018; Li et al., 2019). However, OLTC belongs to mechanical devices, frequent adjustment of OLTC can damage its working life, and OLTC can only adjust voltage non-continuously, resulting in poor flexibility. In addition, due to the integration of renewable energy, the voltage safety margin of the power grid is reduced. Meanwhile, adjusting the voltage for VSL power control will further increase the operational risk of the system (Wu et al., 2022; Zheng et al., 2022).

To solve the above problems, this paper designs a real-time scheduling strategy considering VSLs, and achieves continuous control of access point voltage by adjusting the generators and reactive power output equipment in the network. The innovation points of this paper can be summarized as follows:

- (1) A two-stage evaluation-dispatch model of the VSLs' regulation considering voltage stability constraints is established. This paper fully considers the risk of voltage instability during the VSLs' regulation process. By introducing voltage safety margin (VSM) indicators, safety and reliability of system operation can be guaranteed during the regulation process.
- (2) This paper utilizes the institutional advantages of transmission and distribution coordination in China, and uses the reactive power equipment existing in the system to achieve continuous control of load node voltage, avoiding additional investment and mechanical damage to OLTC.

The framework of this paper is arranged as follows: Section 2 firstly analyzes the electricity consumption characteristics of VSLs, and then designs VSM indicators to ensure the system voltage safety during VSLs' scheduling process; in Section 3, a two-stage method for evaluating the adjustable margin of VSLs is provided,

and real-time control is carried out within the allowable power regulation range. Meanwhile, considering that mathematical model includes non-convex and nonlinear AC power flow constraints and coupling constraints, sensitivity analysis method is used to linearize the expansion at the current operating point to meet the requirements of real-time online computing. Then, in Section 4, the improved IEEE-30 node testing system is used for verification. Finally, Section 5 concludes the whole paper.

## 2 Electricity consumption characteristics analysis of VSLs

### 2.1 Mathematical model of VSLs

In recent years, with the application and popularization of automatic voltage control technology, system operators can achieve voltage control of distribution network feeder nodes by adjusting the reactive power output of generator units in the transmission network. Due to the continuous regulation of reactive power, the shortcoming of OLTC, i.e., discontinuous voltage regulation, is overcome, and the mechanical equipment damage caused by multiple OLTC switching is also avoided. At this point, the VSLs in the main network can be seen as a ZIP load and connected to the transmission network through OLTC.

In previous studies on voltage reduction, energy conservation, and load side frequency response (Wang and Wang, 2014), the ZIP model has been widely used to characterize the relationship between voltage changes and power adjustment in VSLs. This paper mainly considers the real-time steady-state scheduling problem, and the load structure can be considered to remain unchanged in the short term. Therefore, the ZIP model is used to characterize the electricity consumption characteristics of VSLs, which can meet the accuracy requirements of actual scheduling. Its mathematical expression is shown in Eqs 1, 2:

$$\begin{cases} P_{i,t}^L = P_{i,t}^B (a_{i,t}^P k^2 + b_{i,t}^P k + c_{i,t}^P) \\ Q_{i,t}^L = Q_{i,t}^B (a_{i,t}^Q k^2 + b_{i,t}^Q k + c_{i,t}^Q) \end{cases} \quad (1)$$

$$k = U_{i,t}/U_N, \quad i = 1, 2, \dots, N_B \quad (2)$$

Here,  $a_{i,t}^P$ ,  $b_{i,t}^P$  and  $c_{i,t}^P$  represent the coefficients of the quadratic, linear, and constant terms of the active power injected by nodes in the ZIP model, with values of 0.2, 0.3, and 0.5 respectively in this paper.  $a_{i,t}^Q$ ,  $b_{i,t}^Q$  and  $c_{i,t}^Q$  represent the coefficients of the quadratic, linear, and constant terms of the reactive power injected by nodes in the ZIP model, with values of 0.2, 0.3, and 0.5 respectively according to reference (Tang et al., 2018) and this is a typical set of ZIP modeling data for analyzing the scheduling potential of VSLs.  $P_{i,t}^L$  and  $Q_{i,t}^L$  represent the active/reactive injection of load node  $i$  at time  $t$ , respectively;  $U_N$  represents the rated voltage value;  $U_{i,t}$  represents the voltage amplitude of VSL access node  $i$  at time  $t$ ;  $N_B$  represents the number of VSL nodes in the power system.

### 2.2 Calculation method of voltage safety margin (VSM) index

Although continuous control of node voltage can be effectively achieved by controlling the generator units and reactive power

regulation equipment in the transmission network, unreasonable voltage control may affect the safe operation of the system. Meanwhile, the integration of renewable energy such as wind power further reduces the margin for safe operation. Therefore, voltage safety related constraints must be considered in the real-time scheduling process of VSLs. This section designs the voltage safety margin (VSM) index and derives the sensitivity relationship between node power changes and VSM index. The specific mathematical derivation process is as follows:

Firstly, based on the node admittance matrix relationship, establish the system voltage current network equation, as shown in Eq. 3:

$$\begin{bmatrix} \mathbf{I}_G \\ \mathbf{I}_L \end{bmatrix} = \begin{bmatrix} \mathbf{Y}_{GG} & \mathbf{Y}_{GL} \\ \mathbf{Y}_{LG} & \mathbf{Y}_{LL} \end{bmatrix} \begin{bmatrix} \mathbf{U}_G \\ \mathbf{U}_L \end{bmatrix} \quad (3)$$

Here,  $\mathbf{I}_G$  and  $\mathbf{U}_G$  respectively represent the current and voltage vectors of the generator node;  $\mathbf{I}_L$  and  $\mathbf{U}_L$  respectively represent the voltage and current vectors of load nodes. The matrix elements  $\mathbf{Y}_{GG}$ ,  $\mathbf{Y}_{GL}$ ,  $\mathbf{Y}_{LG}$  and  $\mathbf{Y}_{LL}$  can be calculated according to reference (Kessel and Glavitsch, 1986). After matrix transformation, Eq. 3 can be equivalently written in the form shown in Eq. 4:

$$\begin{bmatrix} \mathbf{I}_G \\ \mathbf{U}_L \end{bmatrix} = \begin{bmatrix} \mathbf{Y}_{GG} - \mathbf{Y}_{GL}\mathbf{Y}_{LL}^{-1}\mathbf{Y}_{LG} & \mathbf{Y}_{GL}\mathbf{Y}_{LL}^{-1} \\ -\mathbf{Y}_{LL}^{-1}\mathbf{Y}_{LG} & \mathbf{Y}_{LL}^{-1} \end{bmatrix} \begin{bmatrix} \mathbf{U}_G \\ \mathbf{I}_L \end{bmatrix} \quad (4)$$

Let  $\mathbf{F} = -\mathbf{Y}_{LL}^{-1}\mathbf{Y}_{LG}$ , and the calculation formula for VSM is shown in Eq. 5:

$$\text{VSM}_j = \left| 1 - \sum_{k \in a_G} F_{jk} U_k / U_j \right| \quad (5)$$

It can be observed in Eq. 5 that the VSM index needs to calculate the modulus of the complex number  $1 - \sum_{k \in a_G} F_{jk} U_k / U_j$ . In order to facilitate analysis, the complex term  $\text{VSM}_{C,j}$  is first defined as Eq. 6:

$$\text{VSM}_{C,j} = 1 - \sum_{k \in a_G} F_{jk} U_k / U_j \quad (6)$$

According to the complex modulus calculation rule, Eq. 5 can be transformed into the form shown in Eq. 7:

$$\text{VSM}_j = \sqrt{(\text{Re}(\text{VSM}_{C,j}))^2 + (\text{Im}(\text{VSM}_{C,j}))^2} \quad (7)$$

When the system control variables change, the small change  $\Delta\text{VSM}$  at the current operating point can be calculated according to Eq. 8:

$$\begin{aligned} \Delta\text{VSM}_j &= \frac{\text{Re}(\text{VSM}_{C,j})\Delta\text{Re}(\text{VSM}_{C,j}) + \text{Im}(\text{VSM}_{C,j})\Delta\text{Im}(\text{VSM}_{C,j})}{\sqrt{(\text{Re}(\text{VSM}_{C,j}))^2 + (\text{Im}(\text{VSM}_{C,j}))^2}} \\ &= \frac{\text{Re}(\text{VSM}_{C,j})}{\text{VSM}_j} \Delta\text{Re}(\text{VSM}_{C,j}) + \frac{\text{Im}(\text{VSM}_{C,j})}{\text{VSM}_j} \Delta\text{Im}(\text{VSM}_{C,j}) \end{aligned} \quad (8)$$

The real and imaginary parts of  $\text{VSM}_{C,j}$  are shown in Eq. 9:

$$\begin{aligned} \text{Re}(\text{VSM}_{C,j}) &= 1 - \sum_{k \in a_G} |F_{jk}| U_k / U_j \cos(\delta_{jk} + \delta_k - \delta_j) \\ \text{Im}(\text{VSM}_{C,j}) &= - \sum_{k \in a_G} |F_{jk}| U_k / U_j \sin(\delta_{jk} + \delta_k - \delta_j) \end{aligned} \quad (9)$$

The partial derivative accumulation of state variables, namely, voltage and phase angle, can be obtained as Eq. 10:

$$\begin{aligned} \Delta\text{Re}(\text{VSM}_{C,j}) &= \sum_{k \in a_G} |F_{jk}| U_k / U_j^2 \cos(\delta_{jk} + \delta_k - \delta_j) \Delta U_j \\ &\quad + \sum_{k \in a_G} |F_{jk}| U_k / U_j \sin(\delta_{jk} + \delta_k - \delta_j) \\ &\quad \times (\Delta\delta_k - \Delta\delta_j) \Delta\text{Im}(\text{VSM}_{C,j}) \\ &= \sum_{k \in a_G} |F_{jk}| U_k / U_j^2 \sin(\delta_{jk} + \delta_k - \delta_j) \Delta U_j \\ &\quad - \sum_{k \in a_G} |F_{jk}| U_k / U_j \cos(\delta_{jk} + \delta_k - \delta_j) (\Delta\delta_k - \Delta\delta_j) \end{aligned} \quad (10)$$

Substituting Eq. 10 into Eqs 8, 11 can be obtained:

$$\begin{aligned} \Delta\text{VSM}_j &= \frac{1}{\text{VSM}_j U_j} \text{Re}(\text{VSM}_{C,j}) \sum_{k \in a_G} \text{Re}(F_{jk} U_k / U_j) \\ &\quad + \text{Im}(\text{VSM}_{C,j}) \sum_{k \in a_G} \text{Im}(F_{jk} U_k / U_j) \Delta U_j \\ &\quad - \frac{1}{\text{VSM}_j} \text{Re}(\text{VSM}_{C,j}) \sum_{k \in a_G} \text{Im}(F_{jk} U_k / U_j) \\ &\quad - \text{Im}(\text{VSM}_{C,j}) \sum_{k \in a_G} \text{Re}(F_{jk} U_k / U_j) \Delta\delta_j \\ &\quad + \sum_{k \in a_G} \frac{1}{\text{VSM}_j} \text{Re}(\text{VSM}_{C,j}) \text{Im}(F_{jk} U_k / U_j) \\ &\quad - \text{Im}(\text{VSM}_{C,j}) \sum_{k \in a_G} \text{Re}(F_{jk} U_k / U_j) \Delta\delta_k \end{aligned} \quad (11)$$

Eq. 11 describes the sensitivity relationship between node voltage and phase angle changes and VSM index changes, where  $K$  represents the determinant and matrix elements can be obtained according to Eq. 11. Here, Eq. 11 is written in the compact form shown in Eq. 12:

$$\Delta\text{VSM}_j = \mathbf{K} [\Delta\delta, \Delta U]^T, \mathbf{K} = [\mathbf{K}_1, \mathbf{K}_2] \quad (12)$$

In order to intuitively characterize the impact of node power changes on VSM index, the power flow equation is first introduced here, as shown in Eq. 13:

$$\begin{aligned} \Delta\delta &= \mathbf{M}\Delta\mathbf{P} + \mathbf{N}\Delta\mathbf{Q} \\ \Delta\mathbf{U} &= \mathbf{L}\Delta\mathbf{P} + \mathbf{S}\Delta\mathbf{Q} \end{aligned} \quad (13)$$

The sensitivity relationship between node power variation and VSM index can be obtained by combining Eqs 12, 13, as shown in Eq. 14:

$$\Delta\text{VSM} = (\mathbf{K}_1\mathbf{M} + \mathbf{K}_2\mathbf{L})\Delta\mathbf{P} + (\mathbf{K}_1\mathbf{N} + \mathbf{K}_2\mathbf{S})\Delta\mathbf{Q} \quad (14)$$

### 3 A real-time economic dispatch model for power system based on sensitivity analysis method

When incorporating VSLs into the economic dispatch, as VSLs achieve load power regulation through var-voltage optimization, its economic dispatch includes active power adjustment and reactive power optimization. In summary, the generalized mathematical

model for real-time economic dispatch considering VSLs can be written in the form of Eq. 15:

$$\begin{aligned} \min \quad & H(\mathbf{v}) + G(\mathbf{p}) + F(\mathbf{p}, \mathbf{v}) \\ \text{s.t.} \quad & \mathbf{v} \in \Theta^V: = \{h(\mathbf{v}) \geq 0, \forall \underline{\mathbf{v}} \leq \mathbf{v} \leq \bar{\mathbf{v}}\} \\ & \mathbf{p} \in \Theta^P: = \{g(\mathbf{p}) \geq 0, \forall \underline{\mathbf{p}} \leq \mathbf{p} \leq \bar{\mathbf{p}}\} \\ & \mathbf{v}, \mathbf{p} \in \Theta^{P,V}: = \left\{ \begin{array}{l} f(\mathbf{v}, \mathbf{p}) \geq 0, \\ \forall \underline{\mathbf{v}} \leq \mathbf{v} \leq \bar{\mathbf{v}}, \underline{\mathbf{p}} \leq \mathbf{p} \leq \bar{\mathbf{p}} \end{array} \right\} \end{aligned} \quad (15)$$

Here,  $\mathbf{v}$  and  $\mathbf{p}$  respectively represent variables related to reactive and active power;  $H(\mathbf{v})$ ,  $G(\mathbf{p})$ , and  $F(\mathbf{p}, \mathbf{v})$  represent the objective function terms for reactive power control, active power scheduling, and their coupling part, respectively;  $\Theta^V$ ,  $\Theta^P$ ,  $\Theta^{P,V}$  represent reactive power related constraints, active power related constraints, and coupling constraints, respectively. Due to the existence of reactive power and voltage variables in the objective function, the economic dispatch model based on DC power flow will no longer be applicable. On the other hand, if AC power flow model is adopted, (15) will become a large-scale, nonlinear, and non-convex problem, which is difficult to solve. Due to the fact that VSLs' regulation is based on the current operating point, this paper focuses on sensitivity analysis of the current operating point, thus linearizing the original nonlinear problem to meet the needs of real-time online solving.

### 3.1 VSLs' adjustable margin evaluation method

As mentioned earlier, the regulation of VSLs is mainly achieved through voltage control. During steady-state operation, the adjustable range of voltage at each node is generally allowed to be between 0.95p.u. and 1.05p.u., with the limitation of VSM index, it will further lead to a reduction in the adjustable range of voltage. Therefore, it is necessary to first evaluate the adjustable range of voltage at each node under the current operating point. Corresponding mathematical model for VSLs' adjustable margin evaluation is shown in Eqs 16–23:

$$\text{obj: } \min \sum_{i=1}^{N_B} P_{i,t}^L \text{ and } \max \sum_{i=1}^{N_B} P_{i,t}^L \quad (16)$$

$$\text{s.t. } \begin{bmatrix} \Delta P \\ \Delta Q \end{bmatrix} = J \begin{bmatrix} \Delta \delta \\ \Delta U/U \end{bmatrix} \quad (17)$$

$$\begin{bmatrix} \Delta P_{i,t} \\ \Delta Q_{i,t} \end{bmatrix} = \begin{bmatrix} P_{i,t}^G \\ Q_{i,t}^G \end{bmatrix} + \begin{bmatrix} \Delta P_{i,t}^G \\ \Delta Q_{i,t}^G \end{bmatrix} - \begin{bmatrix} P_{i,t}^S \\ Q_{i,t}^S \end{bmatrix}, i = 1, 2, \dots, N_G \quad (18)$$

$$R_i^{G,d} \leq \Delta P_{i,t}^G \leq R_i^{G,u}, i = 1, 2, \dots, N_G \quad (19)$$

$$\begin{bmatrix} U_{i,t}^{\min} \\ \delta_i^{\min} \end{bmatrix} \leq \begin{bmatrix} U_{i,t} \\ \delta_{i,t} \end{bmatrix} + \begin{bmatrix} \Delta U_{i,t} \\ \Delta \delta_{i,t} \end{bmatrix} \leq \begin{bmatrix} U_{i,t}^{\max} \\ \delta_i^{\max} \end{bmatrix}, i = 1, 2, \dots, N_A \quad (20)$$

$$\begin{bmatrix} P_{i,t}^{G,\min} \\ Q_{i,t}^{G,\min} \end{bmatrix} \leq \begin{bmatrix} P_{i,t}^G \\ Q_{i,t}^G \end{bmatrix} + \begin{bmatrix} \Delta P_{i,t}^G \\ \Delta Q_{i,t}^G \end{bmatrix} \leq \begin{bmatrix} P_{i,t}^{G,\max} \\ Q_{i,t}^{G,\max} \end{bmatrix}, i = 1, 2, \dots, N_G \quad (21)$$

$$\text{VSM} + \Delta \text{VSM} \leq \text{VSM}_{\max} \quad (22)$$

$$\begin{bmatrix} \Delta P_{i,t}^L \\ \Delta Q_{i,t}^L \end{bmatrix} = \begin{bmatrix} 2P_{i,t}^B a_{i,t}^P \frac{\Delta U_{i,t}}{U_N} \\ 2Q_{i,t}^B a_{i,t}^Q \frac{\Delta U_{i,t}}{U_N} \end{bmatrix} + \begin{bmatrix} P_{i,t}^B b_{i,t}^P \frac{\Delta U_{i,t}}{U_N} \\ Q_{i,t}^B b_{i,t}^Q \frac{\Delta U_{i,t}}{U_N} \end{bmatrix}, i = 1, 2, \dots, N_B \quad (23)$$

The objective function (16) and related constraints (17)–(23) construct a VSLs' adjustable range evaluation model. The meaning of objective function (16) is to obtain the lower and upper boundary of the adjustable power of VSLs at the current operating point, in order to ensure the maximum power adjustable range of VSLs; (17) represents the power flow constraint. In (17),  $J$  represents the Jacobian matrix at the convergence of the power flow calculation iteration; (18) represents the balance constraint of active and reactive power at the generator node, where  $\Delta P_{i,t}^G$  and  $\Delta Q_{i,t}^G$  represent the reactive power and active output change of the generator,  $P_{i,t}^S$  and  $Q_{i,t}^S$  represent the active and reactive power of the load connected to the generator node; (19) represents the climbing constraint of generator units, where  $R_i^{G,d}$  and  $R_i^{G,u}$  represents the lower and upper climbing limits of the generator units, respectively; (20) represents the adjustment constraints for node voltage and phase angle and  $N_A$  represents the number of all nodes; (21) represents the active and reactive power output constraints of generator units, respectively; (22) represents the related constraints of VSM index. The system dispatcher ensures voltage safety during the VSLs regulation process by setting a VSM index in advance; (23) represents the linear relationship constraint between active power, reactive power, and voltage in the equivalent ZIP model.

### 3.2 A real-time control model for VSLs

By combining the real-time adjustable range evaluation model of VSLs in Section 3.1, the upper and lower power limits of for VSLs can be obtained. For VSLs' regulation, its essence is to use adjustable VSL resources as flexible backup and supplementary resources for units within the system. Here, the discussion is divided into two scenarios:

Scenario 1: when the actual output of wind power is lower than the short-term forecast value, the power demand on the load side is larger than the sum of the planned output of the units and wind power. If VSLs do not participate in economic dispatch, in order to maintain real-time power balance, it is necessary to increase the output of units in the system or carry out load shedding operations, which increases the operating cost of the system and reduces user satisfaction with electricity consumption. When VSLs participate in scheduling, by reducing the voltage value of VSLs access nodes, the power consumption of VSLs is reduced and real-time power balance is achieved, which is both economical and environmentally friendly.

Scenario 2: When the actual output of wind power is higher than the short-term forecast value, the sum of the planned output of units and wind power is larger than the power demand on the load side. At this time, the conventional operation is to reduce the output of units in the system to maintain real-time power balance. In this case, if VSLs participate in scheduling, power control can be achieved by increasing the voltage of the VSLs' access node. However, there are two drawbacks: Firstly, for the user side, VSLs' regulation is a passive scheduling method. When VSLs' power is increased, it will increase the user's electricity consumption and cost, which is unreasonable; secondly, for the power supply side, increasing VSLs' power to achieve renewable energy consumption has poor economic and environmental benefits. However, in some extreme scenarios, such as when the system communication fails and the output of

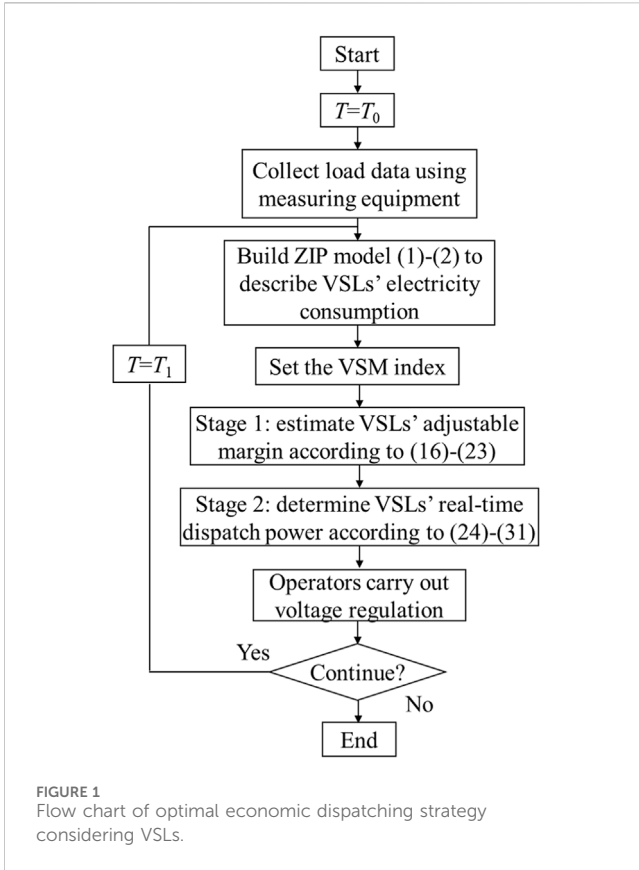


FIGURE 1 Flow chart of optimal economic dispatching strategy considering VSLs.

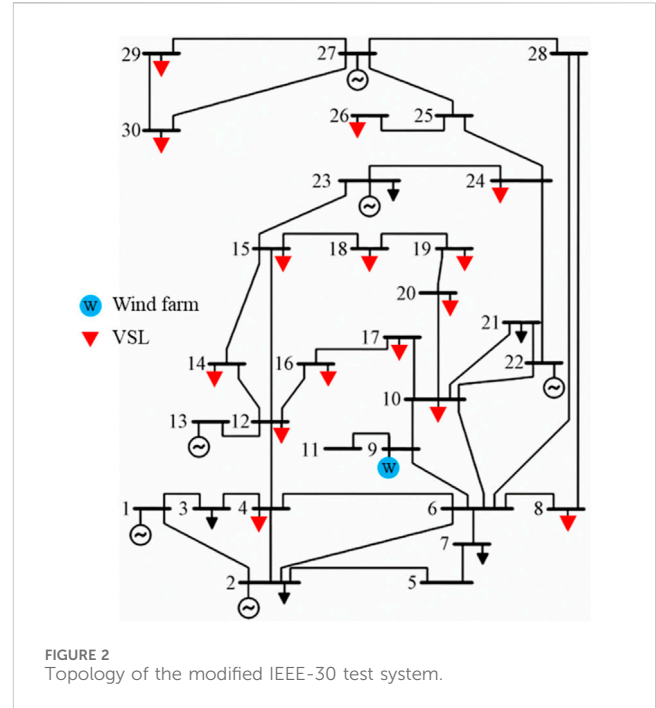


FIGURE 2 Topology of the modified IEEE-30 test system.

the generators cannot be adjusted, it can also be coordinated by increasing the VSLs' power for scheduling. However, the probability of these extreme scenarios occurring is very low. In order to maintain generality, in this paper, the focus is on examining and analyzing the VSLs' scheduling effect under scenario 1.

Based on the adjustable range of VSLs obtained in the previous section, a real-time economic dispatch model can be constructed, as shown in Eqs 24–31:

$$\min \sum_{i=1}^{N_G} P_i^G (P_{i,t}^G) + \sum_{i=1}^{N_B} l^C P_{i,t}^{C,L} + \sum_{i=1}^{N_S} l^C P_{i,t}^{S,L} \quad (24)$$

$$\text{s.t. (17), (19)–(23)} \quad (25)$$

$$\sum_{i=1}^{N_G} P_{i,t}^G + \sum_{i=1}^{N_W} P_{i,t}^W = \sum_{i=1}^{N_B} (P_{i,0}^B + \Delta P_{i,t}^L - P_{i,t}^{C,L}) + \sum_{i=1}^{N_S} (P_{i,t}^S - P_{i,t}^{C,S}) + P_t^{\text{loss}} \quad (26)$$

$$\begin{cases} 0 \leq P_{i,t}^{C,L} \leq P_{i,0}^B + \Delta P_{i,t}^L, i = 1, \dots, N_B \\ 0 \leq P_{i,t}^{C,S} \leq P_{i,t}^S, i = 1, \dots, N_S \end{cases} \quad (27)$$

$$0 \leq P_{i,t}^W \leq P_{i,t}^{W,\max}, i = 1, \dots, N_W \quad (28)$$

$$\begin{bmatrix} \Delta P_{i,t} \\ \Delta Q_{i,t} \end{bmatrix} = \begin{bmatrix} P_{i,t}^G \\ Q_{i,t}^G \end{bmatrix} + \begin{bmatrix} \Delta P_{i,t}^G \\ \Delta Q_{i,t}^G \end{bmatrix} - \begin{bmatrix} P_{i,t}^S - P_{i,t}^{C,S} \\ \tan(\varphi_{i,t}) P_{i,t}^{S,C} \end{bmatrix}, i = 1, 2, \dots, N_S \quad (29)$$

$$\begin{bmatrix} \Delta P_{i,t} \\ \Delta Q_{i,t} \end{bmatrix} = - \begin{bmatrix} \Delta P_{i,t}^L \\ \Delta Q_{i,t}^L \end{bmatrix} + \begin{bmatrix} P_{i,t}^{C,L} \\ \tan(\varphi_{i,t}) P_{i,t}^{C,L} \end{bmatrix}, i = 1, 2, \dots, N_B \quad (30)$$

$$P_{i,t}^{L,\min} \leq P_{i,t}^L + \Delta P_{i,t}^L \leq P_{i,t}^{L,\max}, i = 1, 2, \dots, N_B \quad (31)$$

The objective function (24) represents the minimization of operating costs, consisting of three parts. The first term

represents the operation cost of generator units, which can be calculated based on the quadratic function of the generation cost. The second and third terms represent the cost of load shedding penalty, where  $l^C$  represents the load shedding penalty coefficient and  $P_{i,t}^{C,L}$  represents the load shedding amount of the  $i$ th VSL node at time  $t$ ;  $P_{i,t}^{C,S}$  represents the load shedding amount of the connected load on the  $i$ th generator node; (25) include some constraints that have already appeared in the VSLs' adjustable range evaluation process, including the ZIP model, constraint of VSM index, power flow constraint, generator ramping constraint, generator output constraint, node voltage and angle adjustment range constraints; (26) represents power balance constraint. (27) represents the load shedding range constraint; (28) represents wind power output constraint; (29) represents the power balance constraint of the generator node; (30) represents the power balance constraint of VSLs' nodes; (31) represents the adjustable range constraint of VSLs, where  $P_{i,t}^{L,\min}$  and  $P_{i,t}^{L,\max}$  respectively represent the lower and upper limits of power regulation for the  $i$ th VSL's node at time  $t$ . The specific values can be calculated according to Eqs 16–23.

By combining the current power imbalance deficit and wind power consumption demand of the system, solving models Eqs 24–31 can obtain the optimal VSL control value under the current operating point. To gain a better understanding, a detailed flow chart of optimal economic dispatching strategy considering VSLs is shown in Figure 1.

## 4 Case study

In Section 4.1, the detailed information of the test system is given and the scheduling potential of VSLs and the impact of VSM index are quantitatively analyzed in Section 4.2. Finally, in Section 4.3, two common operating scenarios with different power shortages are given to verify the real-time scheduling value of VSLs.

TABLE 1 Base-state operation active-reactive power of VSL access node.

Node number	Base-state operation point/MVA	Node number	Base-state operation point/MVA
4	7.36 + j1.55	8	28.27 + j28.26
10	5.67 + j1.95	12	10.96 + j7.34
14	5.99 + j1.54	15	7.96 + j2.63
16	3.38 + j1.74	17	8.69 + j5.60
18	3.05 + j0.86	19	9.01 + j3.23
20	2.10 + j0.67	24	8.55 + j6.59
26	3.36 + j2.21	29	2.33 + j0.87
30	10.10 + j1.81		

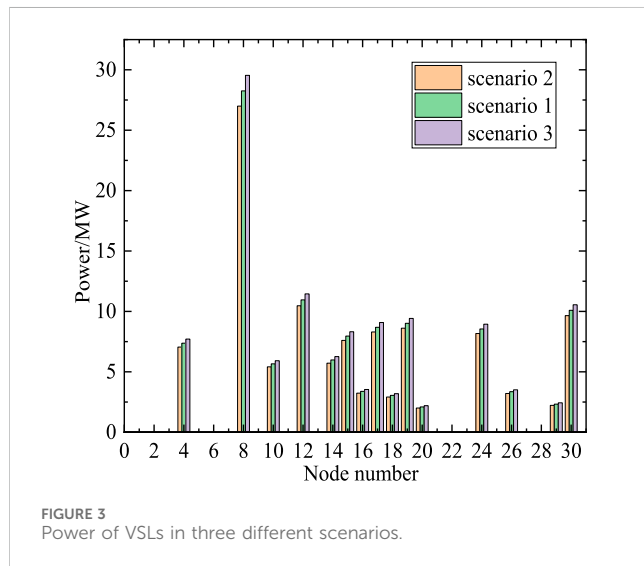


FIGURE 3 Power of VSLs in three different scenarios.

### 4.1 The introduction of testing system

This paper uses an improved IEEE-30 node system for case verification. The testing system topology is shown in Figure 2, and some load nodes are regarded as controllable VSLs (i.e., red triangles in the figure). The power consumption of each VSL is controlled by adjusting the voltage amplitude. The base-state active reactive power of each VSL access node is shown in Table 1. The proposed real-time evaluation scheduling model is written using MATLAB 2016b nested YALMIP and solved using the CPLEX 12.10.0. The desktop computer installed with the software is configured with an Intel TM i5-10400 CPU and a processor of 2.90 GHz.

### 4.2 Adjustable margin analysis of VSLs

This section focuses on analyzing the scheduling potential of VSLs and the impact of VSM index on the regulation range of VSLs. Firstly, Figures 3, 4 respectively show the VSLs' power and corresponding access point voltage in the base-state operation

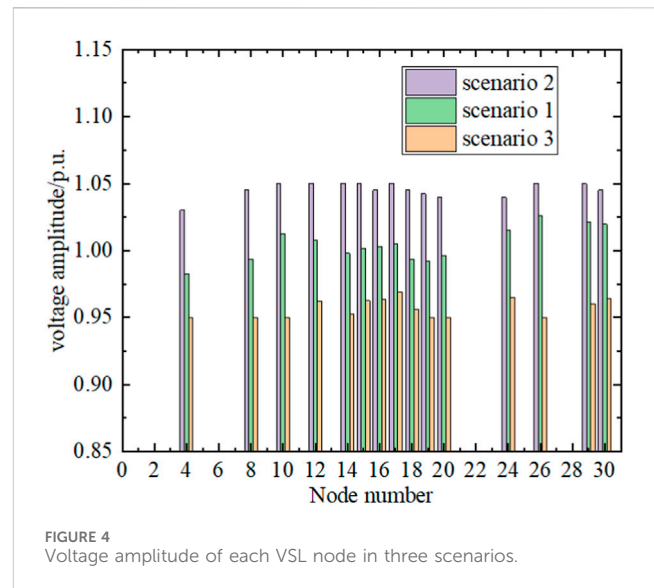


FIGURE 4 Voltage amplitude of each VSL node in three scenarios.

scenario 1, maximizing VSLs' adjustable power scenario 2, and minimizing VSLs' adjustable power scenario 3.

Observing Figures 3, 4, combined with Eq. 1, it can be concluded that the adjustable range of VSLs mainly depends on two factors: firstly, the power of each VSL fluctuates upper and below the base-state operating point, and for VSLs with larger base-state operating power, their adjustable range is often larger; secondly, some nodes have a higher risk of voltage instability, so their voltage adjustable range is smaller, and the controllable power range of VSL is smaller. In order to provide a more intuitive analysis of the scheduling potential of VSL, Table 2 shows the VSLs' power regulation ranges for three different scenarios when the value of VSMmax is 0.15. During maximum upper power operation, the total power of VSL increases by 5.31 MW compared to base-state operation, with a power variation of 4.55%. When operating at maximum lower power operation, the total power of VSLs decreases by 5.20 MW compared to ground state operation, with a power variation of 4.45%. Overall, through voltage control, while ensuring system safety, the newly added regulation range of VSLs accounts for 9% of the total power of base-state operating load, which has great scheduling potential and value. In addition, with the help of reactive power control equipment, node voltage can be adjusted on a second level time scale. The current real-time scheduling time scale in China is 5–15 min, therefore VSLs have a fast response speed and can meet the needs of real-time applications without involving privacy protection issues.

Previously, scheduling strategies for VSLs often ignored the impact of the regulation process on voltage safety (Lauria, 1987; Wang and Wang, 2014). In order to quantitatively analyze the impact of VSM index on the VSLs' power regulation range, Table 3 provides the maximum upper power regulation amount and maximum lower power regulation amount of VSLs under different VSM index.

Under different values of VSM index, the maximum power of VSLs remains basically unchanged, but the maximum power decreases as the value of VSM index decreases. In order to facilitate the explanation of the reasons for this phenomenon,

TABLE 2 VSL power regulation range under three different scenarios when  $VSM_{max} = 0.15$ .

Operation situation	Total power/MW	Power variation/MW	The proportion of power variation
Base-state	116.76	—	—
Maximum upper power operation	122.07	5.31	4.55%
Maximum lower power operation	111.57	-5.20	-4.45%

TABLE 3 VSL power regulation range under different voltage safety margin factors.

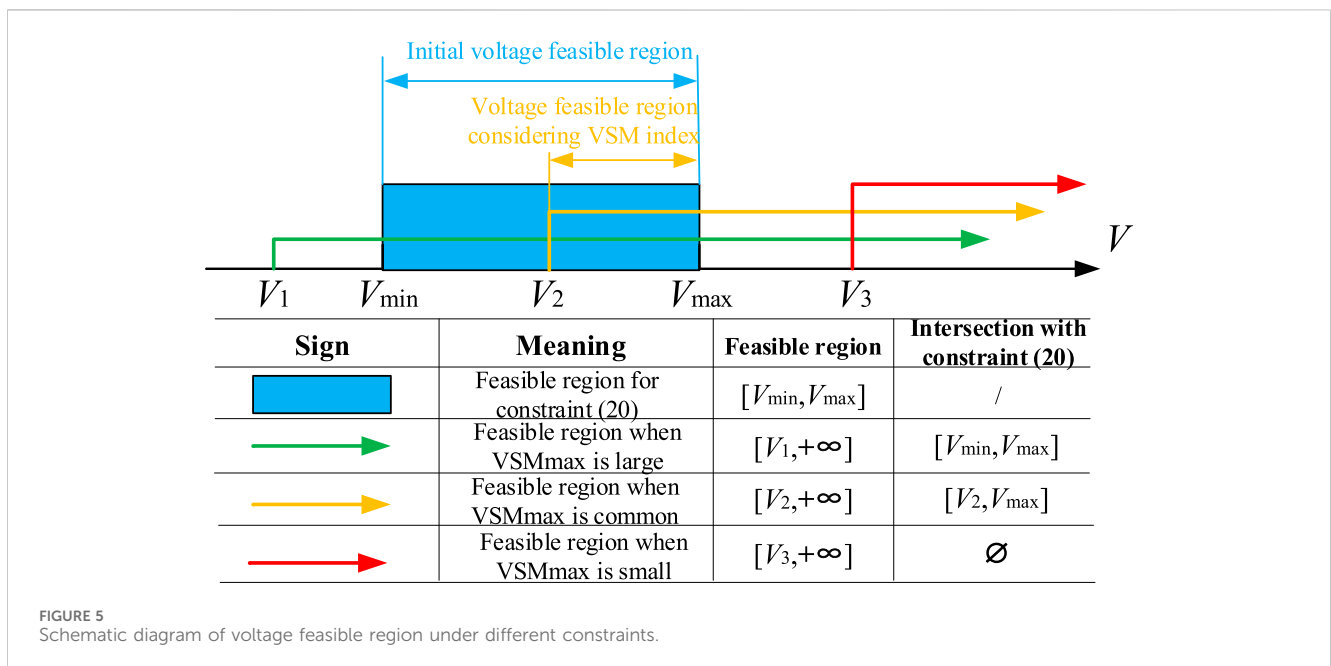
VSM <sub>max</sub>	Maximum upper power adjustment amount/MW	Maximum lower power adjustment amount/MW
0.20	5.31	-5.21
0.15	5.31	-5.20
0.13	5.31	-4.99
0.11	5.31	-4.80
0.09	5.31	-4.67
0.08	5.30	-4.59
0.043	Infeasible	

this time, constraint (22) is ineffective constraint, and the maximum reduction power of VSLs remains unchanged; as the VSM index gradually decreases, both constraints (22) and (20) are effective constraints. The voltage feasible range determined by constraint (22) is  $[V_2, +\infty]$ , which is the yellow line in the figure. The intersection with the voltage feasible range determined by constraint (20) is  $[V_2, V_{max}]$ , indicating that the voltage feasible range is compressed, the lower boundary of the voltage feasible range is raised, and the maximum power reduction of VSLs is reduced. Therefore, for power system dispatchers, the value of the VSM index should not be too small. When its value is too small, the voltage feasible range determined by constraint (22) is  $[V_3, +\infty]$ , as shown in the red line. At this point, the intersection with the voltage feasible range determined by constraint (20) is an empty set, and the optimization problem has no solution. Especially in scenarios with multiple renewable energy inputs and heavy loads, the critical safety value of voltage is already at a high level. In this case, setting a smaller VSM index can easily lead to unsolvable economic scheduling problems. Combined with the data given in Table 3, it can be found that when the VSM<sub>max</sub> value is within the range of [0.15, 0.20], the voltage feasible region is the blue region in Figure 5. In this case, the maximum upper and lower power adjustment amounts remain basically unchanged. When the VSM<sub>max</sub> value is within the range of [0.15, 0.043], the maximum low power adjustment amount gradually decreases. When the VSM<sub>max</sub> value is less than 0.043, there is no feasible solution, indicating that the scheduling decision is too conservative.

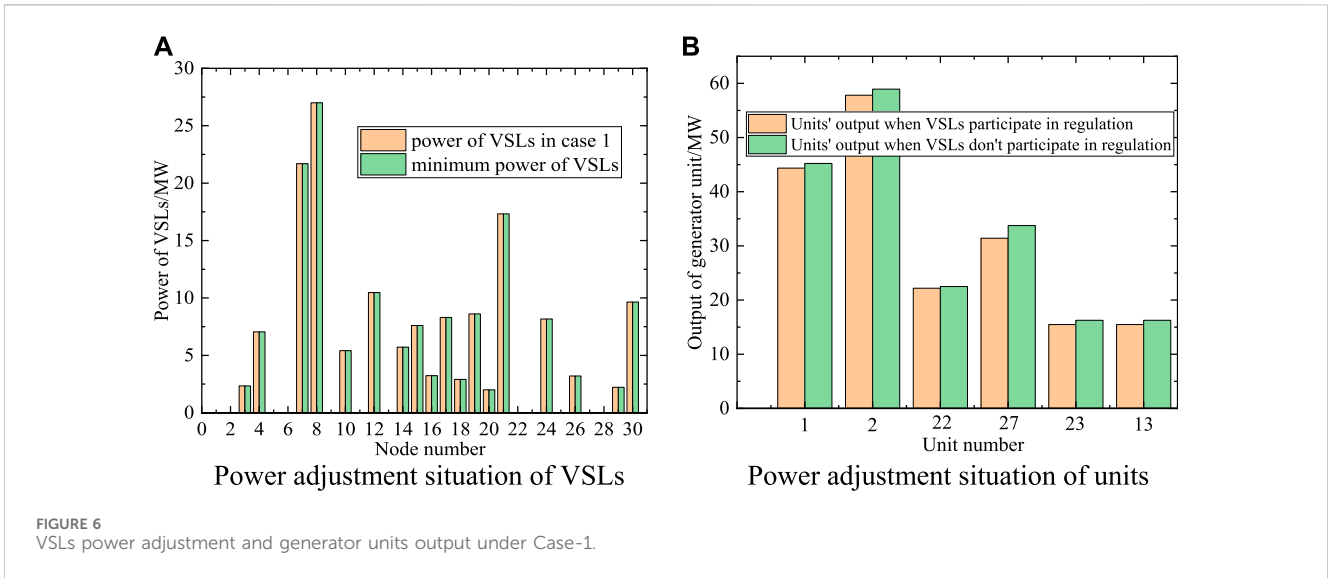
Figure 5 provides a schematic diagram of the voltage feasible region under different constraints. The voltage feasible range of each load node is determined jointly by constraints (20) and (22). The voltage feasible range in the blue area of Figure 5 is determined by constraint (20). When the VSM index is not set in the system or the setting value is large, the voltage feasible range determined by voltage safety constraint (22) is in the right area (i.e., green line in the figure). At

### 4.3 Real-time scheduling benefit analysis of VSLs

In order to provide a more intuitive explanation of the real-time scheduling effect of VSLs, two common operating scenarios with different power shortages have been set up here. The specific information is as follows:

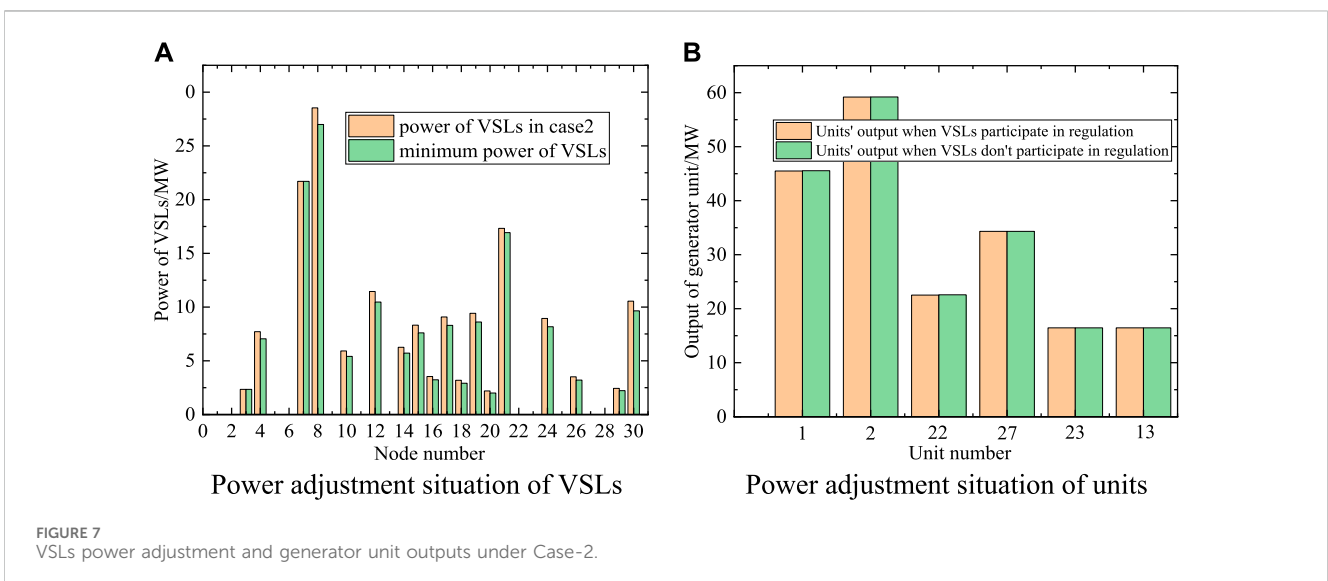






Case 1: Due to the daily prediction error of wind power output and load power, the demand for load side power consumption is 10 MW larger than the sum of the planned output of units and the actual wind power; Case 2: Due to the daily prediction error of wind power output and load power, the demand for load side power consumption is 4 MW greater than the sum of the planned output of units and the actual wind power; In the above two operating scenarios, the power adjustment of VSLs and the output of generator units within the system are shown in Figures 6, 7, respectively. In Case-1, the power shortfall on the power and load sides is 10 MW. Based on Table 2, it can be seen that the maximum reduction power of VSLs under the current operating point is 5.20 MW. This indicates that even when all VSLs' power is adjusted to the minimum value, it is still unable to fill the current power shortfall, and there is a power shortfall of 4.80 MW. Therefore, it is necessary to adjust the units' output in the system to maintain real-time power balance. As shown in Figure 6B, the output of units when VSLs participate in regulation is significantly

lower than that when VSLs do not participate in dispatch. This is because after VSLs participate in dispatch, the real-time power shortfall of the system decreases, and the generator units only need to slightly increase its output to maintain real-time power balance. From the perspective of economic investment, when VSLs do not participate in scheduling, the operating cost under the current point is 579.75 \$. However, when VSLs participate in scheduling, the operating cost of the system decreases to 555.83 \$, which means that the power supply pressure is reduced through VSL regulation, while reducing the cost by 23.92 \$, and avoiding frequent adjustments to the planned output of units. Due to the low base-state operating point of the VSLs, the corresponding adjustable power of VSLs is also small. In heavy load scenarios, the economic benefits brought by VSL regulation will be more considerable. In Case 2, the current power shortfall is only 4 MW, and VSLs' own power adjustment capacity is sufficient to cover the current power shortfall. Therefore, as shown in Figure 7B, there is no need to increase the output of the generator units, which not only ensures



the safe operation of the power system but also reduces operation costs and greenhouse gas emissions. In fact, VSLs' flexibility resources can be seen as virtual generators, serving as backup flexible resources for traditional generator units: increasing VSLs' own electricity consumption is equivalent to reducing the output of units in the system. The evaluation and real-time control process of VSLs is essentially a voltage reduction and energy-saving project that takes into account system voltage safety.

## 5 Conclusion

Considering the real-time power imbalance caused by fluctuations in renewable energy output and prediction errors, this paper proposes a real-time economic scheduling strategy for VSLs. Firstly, considering the power-voltage coupling relationship of VSLs, the ZIP model is used to characterize its electricity consumption characteristics. Meanwhile, the integration of renewable energy and voltage control will further reduce the level of voltage safety. In order to ensure voltage safety during the regulation process, VSM index are designed and included in the VSLs' evaluation scheduling model. Then, considering the non-convex and nonlinear characteristics of the model, a sensitivity analysis method is used to linearize at the current operating point, thus transforming the initial complex nonlinear programming problem into a linear programming problem to meet the needs of real-time online computing. Finally, the scheduling potential of VSLs is verified and analyzed through an improved IEEE-30 node system. Analysis shows that:

- (1) VSL has great scheduling potential. Under the premise of ensuring system voltage safety, the power regulation range of VSLs accounts for about 9% of the total power in the base-state operating scenario;
- (2) The selection of VSM index will have an impact on the control range of VSLs: under different VSM values, the maximum upper regulation power remains basically unchanged, but the maximum lower regulation power decreases as the value of VSM index decreases. For power system dispatchers, VSN index should be reasonably selected to avoid overly conservative decisions leading to unsolvable optimization problems;
- (3) VSLs' flexibility resources can be seen as backup flexibility resources for traditional units. By reducing VSLs' own electricity consumption, it fills the power shortfall in the real-time scheduling stage and reduces the added output of generator units.

## References

- Chen, X., Zhang, Y., Huang, Z., and Xie, S. (2023). Double layer robust economic dispatch of distribution networks and multi microgrids considering node marginal electricity prices. *Power Autom. Equip.* 43 (11), 51–58. doi:10.16081/j.epae.202301004
- Dai, X., Chen, H., Xiao, D., and He, Q. (2022). A review of the application and research of industrial demand response technology in the electricity market environment. *Power Grid Technol.* 46 (11), 4169–4186. doi:10.13335/j.1000-3673.pst.2022.1328
- De Steese, J. (1987). *Assessment of conservation voltage reduction applicable in the BPA service region*. United States: Bonneville Power Administration.
- Diaz, A., Sandraz, J., Macwan, R., de Leon, F., Czarkowski, D., Comack, C., et al. (2013). Field-validated load model for the analysis of CVR in distribution secondary networks: energy conservation. *IEEE Trans. Power Deliv.* 28 (4), 2428–2436. doi:10.1109/tpwr.2013.2271095
- Dwyer, A., Nielsen, R. E., Stangl, J., and Markushevich, N. S. (1995). Load to voltage dependency tests at BC hydro. *IEEE Trans. Power Syst.* 10, 709–715. doi:10.1109/59.387907
- Faddel, S., Sun, Q., and Tian, G. (2022). Modeling and coordination of commercial buildings in distribution systems. *IEEE Trans. Industry Appl.* 58 (2), 1654–1663. doi:10.1109/tia.2022.3145768

## Data availability statement

The original contributions presented in the study are included in the article/Supplementary material, further inquiries can be directed to the corresponding author.

## Author contributions

CZ: Data curation, Methodology, Project administration, Writing–original draft, Writing–review and editing. JJ: Formal Analysis, Methodology, Writing–original draft, Writing–review and editing. CC: Data curation, Methodology, Writing–original draft, Writing–review and editing. HY: Conceptualization, Methodology, Resources, Software, Writing–original draft, Writing–review and editing. DY: Conceptualization, Formal Analysis, Software, Writing–original draft, Writing–review and editing. ZL: Formal Analysis, Methodology, Resources, Writing–original draft, Writing–review and editing.

## Funding

The author(s) declare financial support was received for the research, authorship, and/or publication of this article. This research was funded by Southern Power Grid Co., Ltd. Technology Project “Research and application of cloud edge collaboration and interoperability technology in new power systems,” No. 032000KK52220010.

## Conflict of interest

Authors CZ, CC, and HY were employed by Zhongshan Power Supply Company of Guangdong Power Grid Co., Ltd. Author JJ was employed by Guangdong Power Grid Co., Ltd. Authors DY and ZL were employed by Southern Power Grid Digital Grid Research Institute Co., Ltd.

## Publisher's note

All claims expressed in this article are solely those of the authors and do not necessarily represent those of their affiliated organizations, or those of the publisher, the editors and the reviewers. Any product that may be evaluated in this article, or claim that may be made by its manufacturer, is not guaranteed or endorsed by the publisher.

- Ge, X. (2022). *Research on auction strategy for load side flexibility adjustment resources*. China: Shandong University.
- Herath, P., and Venayagamoorthy, G. K. (2021). Scalable residential demand response management. *IEEE Access* 9, 159133–159145. doi:10.1109/access.2021.3119270
- Jin, H. Y., Li, Z. S., Sun, H. B., Guo, Q., and Wang, B. (2018). A two-stage reactive power optimization in transmission network incorporating reserves from voltage-dependent loads. *Energy* 157, 752–763. doi:10.1016/j.energy.2018.05.112
- Kessel, P., and Glavitsch, H. (1986). Estimating the voltage stability of a power system. *IEEE Trans. Power Deliv.* 1 (3), 346–354. doi:10.1109/tpwrd.1986.4308013
- Kong, X., Wang, Z., Liu, C., Zhang, D., and Gao, H. (2023). Refined peak shaving potential assessment and differentiated decision-making method for user load in virtual power plants. *Appl. Energy* 334, 120609–120618. doi:10.1016/j.apenergy.2022.120609
- Lauria, D. (1987). Conservation voltage reduction (CVR) at Northeast utilities. *IEEE Trans. Power Del.* 2, 1186–1191. doi:10.1109/tpwrd.1987.4308241
- Lezama, F., Soares, J., Canizes, B., and Vale, Z. (2020). Flexibility management model of home appliances to support DSO requests in smart grids. *Sustain. Cities Soc.* 55, 102048. doi:10.1016/j.scs.2020.102048
- Li, D., Zhang, K., Yao, Y., and Lin, S. (2022). A daily demand response scheduling strategy for electric vehicle aggregators based on information gap decision theory. *Power Syst. Prot. Control* 50 (24), 101–111. doi:10.19783/j.cnki.pspc.220181
- Li, G., Liu, G., Hou, L., Jin, L., and Yang, Y. (2019). A quantitative evaluation method for the impact of multiple OLTC coordinated actions on voltage stability. *Power Autom. Equip.* 39 (07), 154–160. doi:10.16081/j.issn.1006-6047.2019.07.023
- Li, W., Han, R., Sun, C., Fu, P., Zhang, J., and Wang, C. (2021). The optimal incentive contract and incentive strategy for shiftable load participation in demand response based on electricity consumption preferences. *Chin. J. Electr. Eng.* 41 (S1), 185–193. doi:10.13334/j.0258-8013.psee.202593
- Lv, S., Ye, L., Li, J., Yang, J., Zheng, C., and Chen, Z. (2018). A medium to long-term voltage stability evaluation index that takes into account the dynamic regulation effect of on load tap changer transformers. *J. Electr. Power Sci. Technol.* 33 (03), 86–92.
- Rassaei, F., Soh, W., and Chua, K. (2015). Demand response for residential electric vehicles with random usage patterns in smart grids. *IEEE Trans. Sustain. Energy* 6 (4), 1367–1376. doi:10.1109/tste.2015.2438037
- Ren, X., Zhang, Z., Xu, L., W, S., Liu, Z., and Xu, F. (2022). Layered energy system optimization scheduling considering the demand response of electric vehicles and temperature control loads. *Electr. Power Constr.* 43 (9), 77–86.
- Schneider, I., Roozbehani, M., and Dahleh, M. (2022). An online learning framework for targeting demand response customers. *IEEE Trans. Smart Grid* 13 (1), 293–301. doi:10.1109/tsg.2021.3121686
- Shi, J., Zhang, Z., Yang, Y., Liu, J., Jiang, Z., and Shan, X. (2022). Design and empirical analysis of building load demand response system scheme. *Power Demand Side Manag.* 24 (3), 60–65.
- Short, T. A., and Mee, R. W. (2012). "Voltage reduction field trials on distributions circuits," in Proc. 2012 IEEE PES Transmission and Distribution Conf. Expo, Orlando, Florida, USA, 7 - 10 May 2012, 1–6.
- Tang, W., Zhang, Y., and Qian, T. (2023). Integrated building cluster distribution network optimization control considering distribution network reconstruction and building cluster active demand response. *Chin. J. Electr. Eng.* 43 (08), 2966–2979.
- Tang, X., Hasan, K., Milanovic, J., Bailey, K., and Stott, S. J. (2018). Estimation and validation of characteristic load profile through smart grid trials in a medium voltage distribution network. *IEEE Trans. Power Syst.* 33 (2), 1848–1859. doi:10.1109/tpwrs.2017.2740563
- Wang, S., Bi, S., and Zhang, Y.-J. A. (2018). Demand response management for profit maximizing energy loads in real-time electricity market. *IEEE Trans. Power Syst.* 33 (6), 6387–6396. doi:10.1109/tpwrs.2018.2827401
- Wang, S., Wang, H., Zhao, Q., Liu, Q., Guo, L., and Zhang, S. (2023). Time of use electricity price optimization method for improving the photovoltaic acceptance capacity of distribution networks. *Power Syst. Autom.* 47 (10), 38–46.
- Wang, Z., and Wang, J. (2014). Review on implementation and assessment of conservation voltage reduction. *IEEE Trans. Power Syst.* 29 (3), 1306–1315. doi:10.1109/tpwrs.2013.2288518
- Wei, Q., Liao, Z., Song, R., Zhang, P., Wang, Z., and Xiao, J. (2021). Self-learning optimal control for ice-storage air conditioning systems via data-based adaptive dynamic programming. *IEEE Trans. Industrial Electron.* 68 (4), 3599–3608. doi:10.1109/tie.2020.2978699
- Wen, L., Zhou, K., Feng, W., and Yang, S. (2024). Demand side management in smart grid: a dynamic-price-based demand response model. *IEEE Trans. Eng. Manag.* 71, 1439–1451. doi:10.1109/tem.2022.3158390
- Wen, Q., Wei, Z., Zhang, Y., Liang, Z., and He, W. (2023). Optimizing operations of electricity selling companies considering insurance mechanisms and user demand response. *Electr. Power Constr.* 44 (1), 47–54.
- Williams, B. (1995). Distribution capacitor automation provides integrated control of customer voltage levels and distribution reactive power flow. *Proc. IEEE Power Ind. Comput. Appl. Conf.* 1995, 215–220.
- Wu, Y., Luo, Y., Lei, C., Huang, Y., Liang, Y., Zhou, S., et al. (2022). Static voltage stability evaluation of power systems containing wind farms based on improved PEM and L index. *China Electr. Power* 55 (09), 192–203.
- Yong, P., Zhang, N., Ci, S., and Kang, C. (2021). 5G communication base station participation in demand response: key technologies and prospects. *Chin. J. Electr. Eng.* 41 (16), 5540–5552. doi:10.13334/j.0258-8013.psee.210183
- Yu, B., Weng, L., Lian, D., Wang, S., Huang, Y., and Yao, H. (2023). A coordinated operation strategy for distributed resource parks that takes into account price guidance mechanisms. *Electr. Power Constr.* 44 (2), 145–154.
- Zeng, X., Yang, P., Liu, L., Yang, K., and Tan, J. (2022). Optimization and control strategies for electric vehicle charging and swapping stations in the electricity spot market environment. *Power Autom. Equip.* 42 (10), 38–45. doi:10.16081/j.epae.202208018
- Zhang, G., Tan, S., and Wang, G. (2018). Real-time smart charging of electric vehicles for demand charge reduction at non-residential sites. *IEEE Trans. Smart Grid* 9 (5), 4027–4037. doi:10.1109/tsg.2016.2647620
- Zheng, L., Ma, D., Zhou, X., and Dai, J. (2022). Research on static voltage stability characteristics of high permeability new energy grid considering SSSC. *Power Demand Side Manag.* 24 (06), 50–56.